Review

Anatomical Factors of the Anterior and Posterior Maxilla Affecting Immediate Implant Placement Based on Cone Beam Computed Tomography Analysis: A Narrative Review

Milica Vasiljevic [1,†], Dragica Selakovic [2,†], Gvozden Rosic [2], Momir Stevanovic [1], Jovana Milanovic [1], Aleksandra Arnaut [1] and Pavle Milanovic [1,*]

1   Department of Dentistry, Faculty of Medical Sciences, University of Kragujevac, 34000 Kragujevac, Serbia
2   Department of Physiology, Faculty of Medical Sciences, University of Kragujevac, 34000 Kragujevac, Serbia
*   Correspondence: pavle11@yahoo.com
†   These authors contributed equally to this work.

Abstract: Background: The aim of this narrative review was to provide insights into the influence of the morphological characteristics of the anatomical structures of the upper jaw based on cone beam computed tomography (CBCT) analysis on the immediate implant placement in this region. Material and Methods:To conduct this research, we used many electronic databases, and the resulting papers were chosen and analyzed. From the clinical point of view, the region of the anterior maxilla is specific and can be difficult for immediate implant placement. Findings: Anatomical structures in the anterior maxilla, such as the nasopalatine canal and accessory canals, may limit and influence the implant therapy outcome. In addition to the aforementioned region, immediate implant placement in the posterior maxilla may be challenging for clinicians, especially in prosthetic-driven immediate implant placement procedures. Data presented within the recently published materials summarize the investigations performed in order to achieve more reliable indicators that may make more accurate decisions for clinicians. Conclusion: The possibility for immediate implant placement may be affected by the NPC shape in the anterior maxilla, while the presence of ACs may increase the incidence of immediate implant placement complications. The variations in IRS characteristics may be considered important criteria for choosing the implant properties required for successful immediate implant placement.

Keywords: morphometric analysis; anterior maxilla; posterior maxilla; immediate implant placement; cone beam computed tomography (CBCT)

1. Introduction

The anatomical border between the anterior and posterior maxilla represents a bony ridge named the zygomaticoalveolar crest. The anterior maxilla is the region that extends from the first premolar on one side to the first premolar on the other side, the cranial border is represented by the anterior nasal opening (the piriform aperture), and the caudal border is the crestal bone [1]. The benefits of cone beam computed tomography (CBCT) usage in planning interventions in the anterior maxilla region have been confirmed in planning implant placement, especially regarding the existence and type of nasopalatine (NPC) and accessory canals (ACs). Also, the importance of CBCT image analyses has been reported in planning interventions in the maxillary molar region. The advantages of such a diagnostic procedure were highlighted in the sense of interradicular septum (IRS) morphological characteristics analysis, which allows for reliable planning of implant therapy.

The use of CBCT imaging in medicine evolved in the 1980s, which was followed by its introduction in dentistry during the 1990s [1]. CBCT is an extraoral radiographic technique that provides a precise 3D image of hard-tissue structures. CBCT imaging is based on the use of a rotating gantry carrying a source of X-ray radiation and a detector.

A divergent cone-shaped source of radiation passes directly across the field of interest, and the remaining attenuated radiation is beamed onto the X-ray detector surface on the other side [2,3]. In order to make full volume of the image, only one rotation around the patient is necessary [4]. It is well-known that a significant improvement in the analysis of this maxillary region was achieved by using CBCT. The use of CBCT has overcome the deficiencies of other radiological methods, such as the distortions and superimpositions of 2D radiography, poor resolution, the limited access of computed tomography, the high cost, difficulties in interpretation in dentistry, the longer scanning time, disturbances of metal artifacts, and the high radiation exposure of computed tomography and multi-sliced computed tomography [3]. The use of the CBCT methodology has already been proven to have remarkable characteristics for the subtle morphometric analysis of structures that may be of potential interest in planning the procedures accompanied by immediate implant placement [3,4].

The work's methodology results in multiplanar views of the dento-maxillofacial region [5]. Also, CBCT provides primary image reconstruction in three fundamental orthogonal planes (Figure 1), such as axial, sagittal, and coronal [6]. Furthermore, the advantages of CBCT analysis provide across-sectional (individual plane) evaluation. It has an importance in the estimation of non-symmetrical structures, such as maxillary sinus septa and alveolar ridge dimensions [7,8]. As the radiation dose in conventional CT and MSCT imaging is up to 10 times higher than in CBCT, CBCT has primacy in the examination of anatomical structures [9]. In addition to the mentioned preference, there are many other advantages, such as the sub-millimeter resolution (2 line pair/mm), images of higher diagnostic quality, shorter scanning times (~60 s), minimal distortion and reduced radiation dosage [2], as well as lower cost than the CT/MSCT [10].
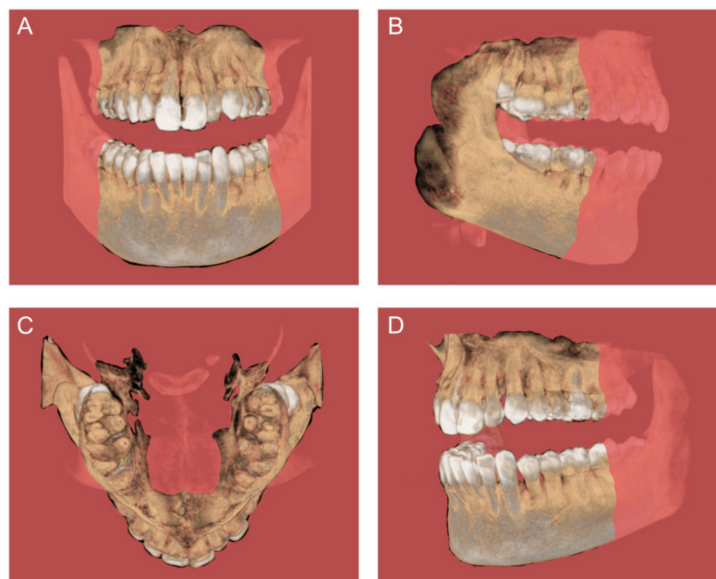
Figure 1. CBCT images with the orthogonal planes: (**A**) coronal, (**B**) sagittal, (**C**) axial, and (**D**) individual plane.

From the clinical point of view, knowledge of anatomical structures and their spatial relationships is crucial in medicine and dentistry for diagnosis and treatment planning [11,12]. Oral and maxillofacial surgery, implantology, orthodontic, ophthalmology, and otorhinolaryngology are fields with increased usage of CBCT [13–17]. The indications for using CBCT have been established by numerous international associations (the Swiss Association of Dentomaxillofacial Radiology and the American Academy of Oral and Maxillofacial Radiology [18,19]). The evaluation of nasopalatine canal (NPC) morphometric characteristics is highly recommended in immediate implant placement planning [20]. Furthermore, CBCT is a reliable radiographic tool used to simulate clinical situations (implant placement)

using virtual implants so as to prevent complications [21,22]. Also, virtual planning in maxillofacial surgery is impossible without 3D imaging, and it has been confirmed that CBCT has become a pillar in the design of therapy and in the navigation-based guidance of surgeons during procedures [23–26]. Furthermore, CBCT scans could allow for navigation implantology, so it is currently considered the gold standard for implant site estimation and treatment planning [27]. The study by Nickenig and collaborators [28] has confirmed that navigation implant placement using CBCT and surgical guides may provide successful implant therapy. It leads to the following advantages: a more precise implantation site, the protection of anatomical structures, high geometrical accuracy, being less invasive, shorter treatment and surgery periods, flapless surgery, and, consequently, less possibility of swelling [29]. Furthermore, 3D bone estimation is recommended for numerous procedures, such as preoperative surgical planning for computed assisted surgeries of tumors and traumas, ridge preservation [30], sinus floor elevation [31,32], and implant placement with bone augmentation [33,34] or phased procedures following block grafts [35–38].

Therefore, the aim of this narrative review was to highlight recent findings regarding the advantages of using the CBCT methodology in the evaluation of the maxillary region and its specific morphometric characteristics with clinical importance.

2. Materials and Methods

Our investigation used the electronic scientific resources PubMed, Scopus, and additional sources, such as Google Scholar and major journals. The search was supplemented with a manual search based on the reference lists of the selected papers and other previous reviews including related journals. Inclusion criteria were studies discussing morphological and morphometric characteristics of NPC, ACs, and IRS using CBCT. Only English-language articles were reviewed. Exclusion criteria included studies with patients under the age of 18. Scientific data were searched during the period between 1 January 2008 and 1 July 2024 to identify primary articles utilizing keywords: "cone beam computed tomography" OR "cone beam CT" OR "CBCT" AND nasopalatine canal OR NPC, accessory canals OR ACs, interradicular septum OR interradicular septal bone OR IRS OR ISB, anterior maxilla OR premaxilla OR alveolar ridge OR posterior maxilla, maxillary central incisors OR MCIs. Those studies that fulfilled the selection criteria were processed for data extraction. After extensive searching, a total of 115 studies were identified and underwent title and abstract screening, and then 61 studies were selected for full-text screening. After full-text screening, 24 studies were excluded. Hence, a total of 37 studies that met our inclusion criteria were processed for data extraction (Figure 2).
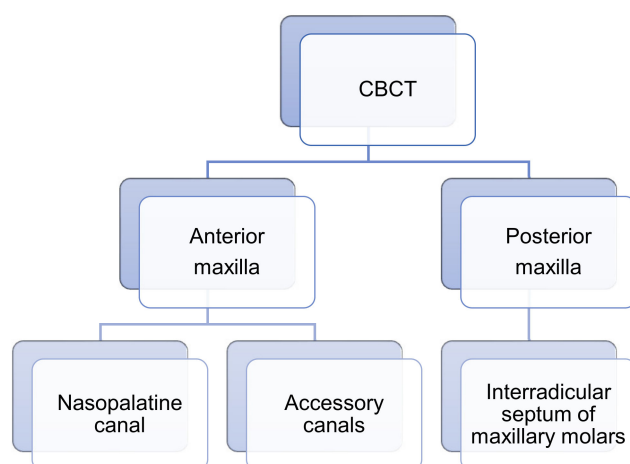

Figure 2. The scheme of the analyzed anatomical structures of the anterior and posterior maxilla through CBCT.

3. Benefits of CBCT Usage in Planning the Interventions in the Anterior Maxilla Region

Recent studies [13,14] performed using morphometric analyses of CBCT images in the anterior maxilla region performed in order to improve the planning of surgical interventions in that region identified NPC and ACs as potential morphological key structures for the final outcome.

It is well-known that the most prominent anatomical structure in the anterior maxilla is the NPC, the content of which is already described [21,39–42]. In addition, Mardinger and coworkers [43] classified NPC shapes in four categories, as follows: cylindrical-, funnel-, banana-, and hourglass-shaped.

Distribution of NPC shapes in the study by Mardingler and collaborators [43] was cylindrical, funnel, hourglass, and banana (Figure 3) (50.7, 30.9, 14.5, and 3.9%, respectively). However, Fukuda and coworkers [44] reported the following distribution: funnel, cylindrical, hourglass, and banana (50, 45, 5, and 0%, respectively). Gil-Markques and colleagues [45] noticed that 32.5% of NPCs were banana-shaped, while cylindrical and funnel shapes appeared in 23.5%, while hourglass was the least represented with 20%. In addition, de Lima and coworkers [46] found that the funnel NPC shape was the most frequent, followed by cylindrical, hourglass, and banana NPC shapes (34.1, 27.5, 25.1, and 13.3%, respectively). Recent studies by Milanovic [14] and Arnaut [13] described similar NPC shape distribution. Namely, Milanovic and colleagues [14] noticed that funnel was 35.4%, cylindrical 31%, hourglass 24.8%, and banana 8.8%. Furthermore, Arnaut and coworkers [13] reported that funnel was the dominant NPC shape (34.59%), followed by cylindrical, hourglass, and banana (28.57%, 24.89%, and 12.03%, respectively).
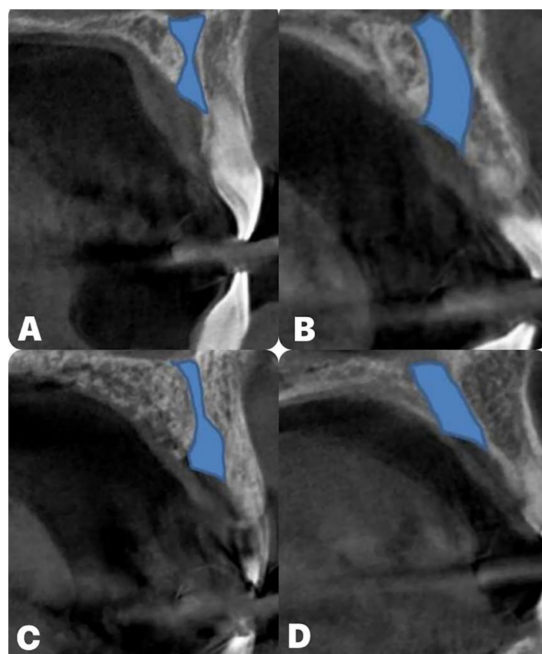
Figure 3. The different NPC types: (**A**) hourglass; (**B**) banana; (**C**) funnel; (**D**) cylindrical.

In addition, numerous studies [43–47] examined dimensions of NPC (NPC length, the diameter of incisive foramen, and the nasal foramen diameter). Thus, Mardinger and coworkers [43] noticed that the mean NPC length was 10.7 mm, while the diameters of the incisive foramen and the nasal foramen were 2.94 mm and 2.55 mm, respectively. Etoz and colleagues [47] reported that the mean NPC length and the incisive and the nasal foramen diameter were found at average levels of 12.59 mm, 5.06, and 3.09 mm, respectively. In addition, Fukuda and collaborators [44] quantified the NPC length and the incisive and the nasal diameters as 11.75 mm, 4.28 mm, and 2.84 mm, respectively. Similarly, de Lima

and coworkers [46] presented an NPC length of 12.67 mm, while the incisive foramen and the nasal foramen diameters were 3.49 mm and 2.89 mm, respectively.

Furthermore, we analyzed studies that examined the horizontal dimension of the anterior maxilla at different levels that corresponded to postponed NPC [14,39,45]. Thus, Bornstein and colleagues [39] evaluated the horizontal dimension of the anterior maxilla at three consecutive levels. At the lowest level, they observed the minimal dimension of buccal bone wall (6.5 mm) that was followed by the dimension at the middle level (6.59 mm), while the highest thickness (7.6 mm) was observed at the highest level. Gil-Markques and coworkers [45] also measured the horizontal dimension of the anterior maxilla (central incisors region) at three levels and confirmed the same algorithm: the thickness of the buccal bone increased stepwise according to the level of elevation (6.8, 7.2, and 9.9 mm, respectively). On the other hand, Milanovic and collaborators [14] analyzed the horizontal dimension of the anterior maxilla at four consecutive levels (A, B, C, and D) and reported the nonlinear dimensions' increase (7.11, 7.03, 7.52, and 9.22 mm, respectively). However, only the study by Milanovic and coworkers [14] statistically evaluated the relationship between NPC shape and the horizontal dimension of the anterior maxilla. That methodological approach was used for defining the potential criteria for immediate implant placement in the region of the maxillary central incisors. Severe criteria for expected success are demanded in implant therapy, so it seems necessary to evaluate the morphometric characteristics of the implant site prior to intervention. Hence, Botermans and colleagues [48] recommended the criteria for immediate implant placement in the maxillary esthetic zone. Namely, they proposed that the minimum distances from the labial and palatal bone plates should be 2 mm each. Also, Milanovic and colleagues analyzed the anterior maxilla in the region of the central incisors and gave potential checkpoints in the immediate implant placement planning [14]. Furthermore, the most critical point (insufficient alveolar bone dimension) for the fulfillment of requirements for successful implant therapy was observed in the banana NPC shape. Following the minimal implant diameter (3 mm, [48]) for central incisors immediate implant placement, we present the available bone according to the NPC shape in Table 1.

Table 1. Available bone dimension for the implant placement in the anterior maxilla according to the NPC shape (in mm). Insufficient space (marked in red); minimal required dimensions (marked in yellow); sufficient space (marked in green).

The Horizontal Dimensions of the Anterior Maxilla at Different Levels	NPC Shape			
	Banana	Hourglass	Cylindrical	Funnel
Level A	2.3	3.2	2.9	3.5
Level B	1.4	3.4	3.2	3
Level C	1.6	4	3.6	3.7
Level D	2	5.9	5.7	5.8

Other neurovascular structures in the anterior maxilla analyzed for their potential importance in this narrative review were ACs. Numerous studies estimated morphological and morphometric characteristics of ACs [49–57]. However, the reported data for the presence of ACs were variable. Thus, Machado [51] reported an incidence of 52.1% and Vasiljevic [49] reported 49.23%, while Baena-Caldas [50] reported that ACs were present in all patients. On the other hand, de Oliveira-Santos [57] observed the presence of ACs in only 15.7%.

In addition, according to ACs' direction, von Arx and coworkers [52] described three AC shapes (Figure 4) and noticed that the incidence of the curved AC shape was 56.7%, while vertical and Y AC shapes were present in 41.79% and 1.51%, respectively. Tomrukcu and colleagues [53] reported that the curved shape was even more frequent (69.15%) when compared to vertical and Y AC shapes (26.16 and 4.67%). In a study by Vasiljevic and

collaborators [49], the prevalence of AC shapes was 48.96%, 36.45%, and 14.58% (curved, vertical, and Y-shaped, respectively).
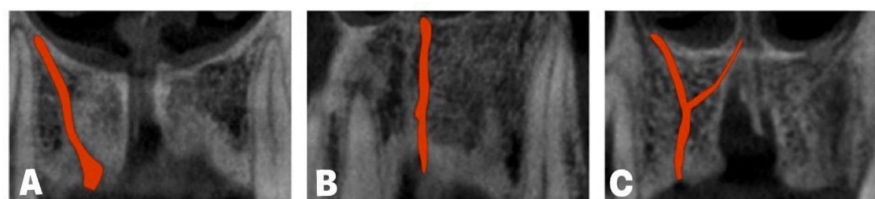
**Figure 4.** Accessory canal shapes: (**A**) curved; (**B**) vertical; (**C**) Y-shape.

Numerous studies estimated AC diameters [49,51,53,57] and confirmed that the mean diameter of ACs was approximately 1–1.5 mm. However, the evaluation of the distance between maxillary central incisors and ACs was performed only in the study by Vasiljevic and coworkers [49]. That analysis also provided insight into the relationship between NPC shape and the distance between ACs and maxillary central incisors.

As mentioned above, although not evaluated to the extent of NPC, another anatomical structure that could have an impact on immediate implant placement in the maxillary central incisors region is the AC. The recommended ideal implant position in the anterior maxillary extraction socket is the apico-palatal guiding slot technique (2 mm below the apex of the extraction socket [58]). At the same time, a proposed safety zone of 2 mm from the implant position to the bundle was recommended by Greenstein and colleagues [59]. According to the literature data, it is obvious that ACs' presence may be considered as a limiting factor for immediate implant placement in the region of maxillary central incisors [59–61]. In order to reacha compromise in the recommended data, it is clear that in Table 2 it is quantitatively confirmed that the existence of ACs should be considered as excluding criteria for the implant placement.

Table 2. Average palatal distance between accessory canals (ACs) and maxillary central incisors (MCIs) for implant placement according to NPC shape (in mm). Insufficient distance marked in red.

ACs–MCIs Distance at the Different Levels	NPC Shape			
	Banana	**Hourglass**	**Cylindrical**	**Funnel**
Level A	1.18	0.9	0.8	1.05
Level B	1.19	1.1	1.08	1.17
Level C	0.8	1.25	1.7	1.3

Finally, based on all morphometric measurements obtained from CBCT images in numerous studies [13,14,49], provisional guidelines were proposed for the immediate implant placement according to the NPC shape and ACs' presence (Figure 5).
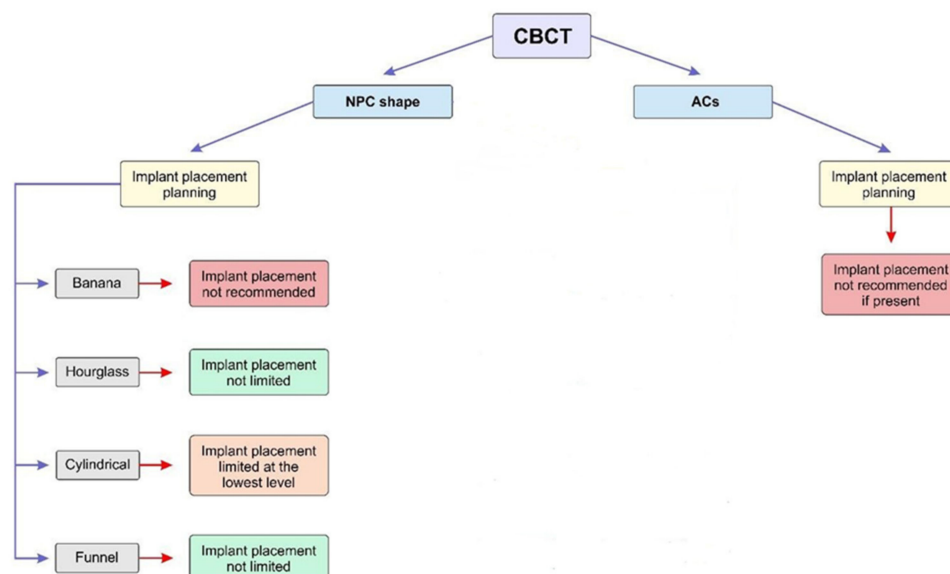
Figure 5. Proposed recommendations for implant placement according to the NPC shape and ACs present. Recommendations for implant placement are based only on the morphometric characteristics without additional interventions (ossedensificaton, bone grafting, and NPC exploration).

4. Benefits of CBCT Usage in Planning the Interventions in the Maxillary Molar Region

From the aspect of the posterior maxilla, IRS presents the ideal place for implant placement, and it is not surprising that numerous studies estimated morphological IRS characteristics [62–66].

A recent study considering IRS [62] presented morphological and morphometric IRS maxillary molar characteristics at the predefined levels using sagittal and axial CBCT slices. There were no significant differences (sagittal slices) reported between IRS characteristics of the maxillary molars (both) in bilateral comparison. The same confirmation was noticed using axial CBCT slices. In addition, differences between IRS characteristics of the first and second maxillary molars were evaluated. Namely, using sagittal CBCT slices, we concluded that the interradicular septum width of the first molars was significantly higher when compared to the second maxillary molars at all evaluated IRS height levels. The same results were reported for the interradicular furcation angle. On the other hand, the IRS height of the second molars was significantly higher than the IRS of the first molars (7 mm and 6.5 mm). Agostinelli and coworkers [66] reported a higher value for the IRS height of the first maxillary molars compared to the second (4.51 vs. 3.24 mm). Finally, no significant difference was shown in the distance between the IRS base and the sinus floor of the first and second molars.

Furthermore, using axial CBCT slices, the perimeter and IRS surface area of the first and second molars were estimated [63]. The average first maxillary molars' perimeter and surface area values were app. 11 mm and 5.5 mm^2 at the lowest level, with stepwise increases in perimeter (12.5, 14, and 16 mm) and surface area (8, 9, and 12.5 mm^2) in the higher sectors. The IRS perimeter and surface area of the second maxillary molars were significantly lower when compared to the first molars. Again, from the bottom to the top, a stepwise increase was observed both for the perimeter (7.5, 10, 11, and 13 mm) and the surface area (3, 4.5, 5.5. and 6.5 mm^2) of the second maxillary molars. A similar observation was reported by Agostinelli and colleagues [66].

Because a possible relationship between different anatomical structures was noticed in previous studies [13,14], the interconnection between the IR furcation angle and the IRS surface area/height at level A for both maxillary molars was estimated. Namely, the correlation between the IR furcation angle and the IRS surface area at level A was

significantly positive, while it revealed a significant negative correlation between the IR furcation angle and the IRS height for both groups of molars [63].

This was soon followed by a recent study [63], which proposed the classification of the IRS structure into five different shapes (arrow-, boat-, drop-, palatal-convergence-, and buccal-convergence-shaped) based on coronal CBCT slice analysis (Figure 6). This classification resulted in predefined quantitative criteria for maxillary molars' IRS. The maxillary molars' IRS widths at the base level for the arrow, boat, palatal, and buccal convergence were ≥4 mm. In contrast, for the drop IRS shape, the IRS width was ≤4 mm, which was also the case for both maxillary molars. The second (and final) principal criterion for IRS shape classification was the IR furcation angle. The first molars' IR furcation angles for the arrow and palatal convergence shapes were ≤60° and ≤70°, respectively. On the other hand, the IR furcation angle of buccal convergence, drop, and boat IRS shapes were ≥60°, ≥70°, and ≥90°, respectively. Less variability in the IR furcation angle was shown in the second molars. Hence, the arrow, drop, palatal, and buccal convergence shapes presented IR furcation angles ≤70°, while in the boat IRS shape the angle was ≥70°. It was also noticed that the most frequent IRS shape was arrow (app. 45%), while the lowest frequency was observed for the drop-shaped IRS (app. 11.5%). Similar variability in IRS shapes' appearance was present in both the first and the second maxillary molars.
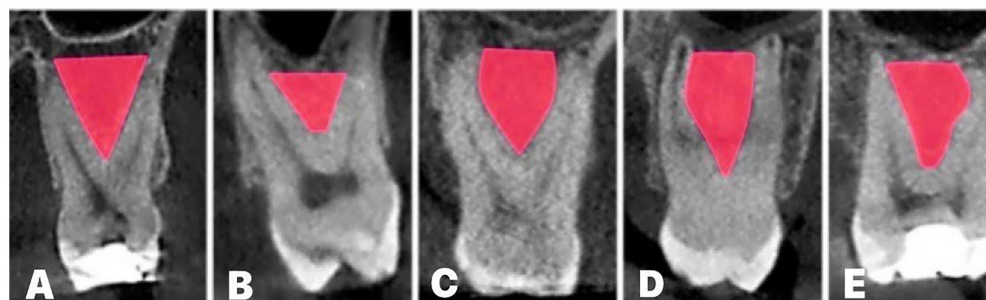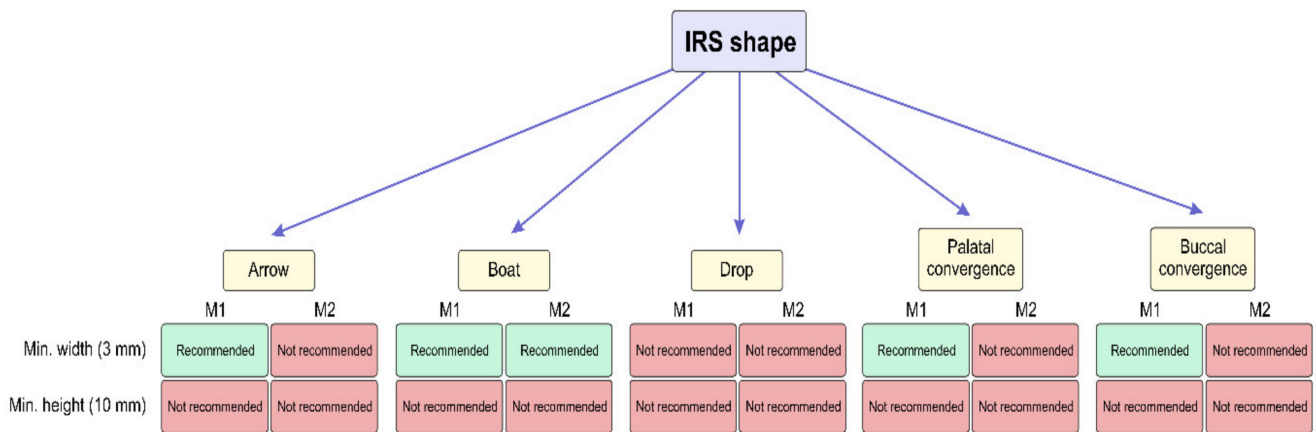

Figure 6. Maxillary molars' IRS shapes:(**A**) arrow; (**B**) boat; (**C**) drop; (**D**) palatal convergence; (**E**) buccal convergence.

In the same study [63], the IRS shape significantly affected all examined parameters (IRS width at the different levels, IR furcation angle, IRS height, distance between IRS base and sinus floor, distance between IR furcation and sinus floor, as well as IRS surface area at all estimated IRS levels). For the first maxillary molars, at all evaluated IRS levels obtained on the coronal view, palatal convergence showed the highest value for the IRS width, as well as height. Afterwards, the IR furcation angle expressed the highest values in the boat shape. This shape also expressed the smallest distance between the IR furcation and the sinus floor. For the second molars, the drop-shaped IRS presented the narrowest IRS at all estimated levels, but with the highest septum. The same was true for the first molars;the largest angle and the smallest distance between the IR furcation and the sinus floor were in the boatshape for the second molars.

Finally, the results obtained on axial slices [63] confirmed that the largest IRS surface area (at all estimated levels) was in the palatal convergence IRS shape for the first upper molars group. Interestingly, the results of the same study showed that the variations in the IRS surface area for the second molars were more prominent, as the highest values for the IRS surface area were observed at the different IRS heights for various IRS shapes.

Also, several authors gave recommendations for IRS dimensions (minimum width of 3 mm and height of 10 mm) for successful immediate implant placement [67,68]. According to this recommendation, we give a suggestion for immediate implant placement based on IRS shape morphometric characteristics [63] in Figure 7. On the other hand, some interventions, such as ossedensification and crestal sinus lift, can overcome this limitation. Namely, both IRS ossedensification and crestal sinus lift elevation can be performed in one-stage surgery. Numerous studies confirmed high rates of success of this intervention [69,70].

IRS shape

	Arrow		Boat		Drop		Palatal convergence		Buccal convergence	
	M1	M2	M1	M2	M1	M2	M1	M2	M1	M2
Min. width (3 mm)	Recommended	Not recommended	Recommended	Recommended	Not recommended	Not recommended	Recommended	Not recommended	Recommended	Not recommended
Min. height (10 mm)	Not recommended	Not recommended	Not recommended	Not recommended	Not recommended	Not recommended	Not recommended	Not recommended	Not recommended	Not recommended

Figure 7. Proposed implant placement recommendations according to the morphometric characteristics depending on IRS shape (without additional surgical treatment).

In addition, following the even more rigorous criterion, based on the fact that the most commonly used implant diameter in the posterior maxilla is 4 mm [69,70], in Figure 8, an overview is presented confirming that none of IRS shapes provides sufficient space for reliable implant placement stability. The proposed analysis is in line with the previous report that described difficulties with immediate implant placement into IRS [71].

IRS shape

	Arrow		Boat		Drop		Palatal convergence		Buccal convergence	
	M1	M2	M1	M2	M1	M2	M1	M2	M1	M2
Implant diameter (4 mm)	Not recommended	Not recommended	Not recommended	Not recommended	Not recommended	Not recommended	Not recommended	Not recommended	Not recommended	Not recommended
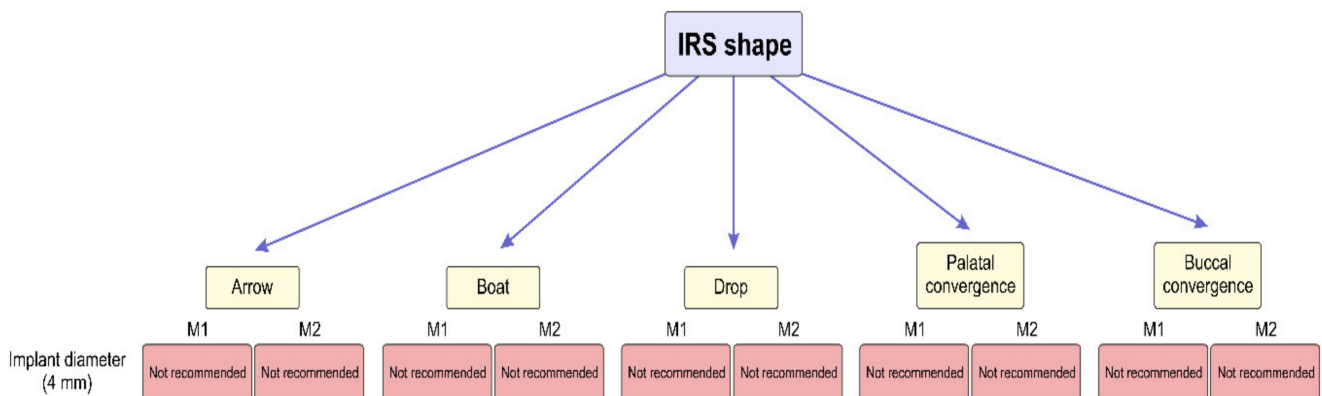
Figure 8. The analysis of IRS morphometric potentials required for reliable implant placement stability according to the IRS shape. (Proposed recommendations for the implant placement are based only on the IRS morphometric characteristics without additional surgical treatment).

5. Discussion

As it is already known, CBCT provides precise bone measurements in order to prevent complications during interventions in the anterior maxilla [13,14]. One of the main criteria for successful immediate implant placement in the region of maxillary central incisors is sufficient thickness of the labial alveolar bone [72]. Thus, some authors [73,74] reported that labial alveolar bone thickness should be at least 2 mm to avoid labial gingival recession and so that biological and esthetic outcomes are achieved. In addition, CBCT examination of the alveolar ridge inclination during implant planning therapy is highly recommended [20]. Namely, immediate implant placement in the region of the anterior maxilla, especially in the lateral incisors area, could be compromised by facial bone concavity [75–77].

On the other hand, it has been confirmed in recent studies that anatomical structures in the anterior maxilla, such as the NPC and accessory canals (ACs), could also compromise interventions in that region [21,49]. It is not surprising that numerous studies performed using CBCT images' morphometric analyses in the anterior maxilla region with the aim to improve the planning of surgical interventions in that region pointed to the NPC and ACs as potential morphological key structures for the final outcome [13,14].

Several NPC morphological classifications have been proposed in the current literature data [43,47,78,79].Milanovic and collaborators evaluated the dimensions of the alveolar bone (as the common place for NPC and AC appearance) andthe thickness at the four consecutive height levels and concluded that the inferior parts of the anterior maxilla presented a lesser dimension than the superior parts [14]. Their findings were in line with the previous observations by Güncü [80] and Lopez and collaborators [81]. A recent study [14] estimated the impact of NPC shape on the anterior maxilla dimensions and confirmed that the impact existed. Namely, except at the lowest level, patients with the banana NPC shape had the smallest horizontal dimension of the anterior maxilla [14].

In order to achieve adequate morphometric conditions for immediate implant placement, especially in patients with a banana NPC shape, several additional surgical interventions (such as bone augmentation and NPC exploration) have been proposed [82,83]. Also, using the NPC as an implant place can be considered [84]. Furthermore, it was suggested by Singhal and coworkers [85] to use surgical guides for precise implant placement into nasopalatine foramen. In patients with funnel NPC shapes, simultaneous use of surgical guides during implant insertion has been recommended [86].

In contrast to the commonly accepted opinion that the NPC is the only neurovascular structure in the anterior maxilla with clinical importance [87], the importance of the estimation of the additional existing channels was highlighted in recent studies [49,50]. A recent study [49] confirmed that the ACs were present in the region of the maxillary central incisors in 49.23% of patients, which is in line with von Arx and colleagues [52], while Wanzeler and collaborators found ACs in almost 90% [54]. Bilateral localization was reported as the most frequent in estimation of ACs' localization by Anatoly and coworkers [55], which is in accordance with our previous study [49]. On the other hand, Manhães and collaborators showed that the variations in AC distribution were side-dependent [56]. Machado [51] and Vasiljevic and coworkers [49] also evaluated ACs' diameter and showed that it was approximately 1 mm, while Oliveira Santos and colleagues [57] reported a slightly larger AC diameter.

Furthermore, there are numerous studies that assessed the interconnection between NPCs and ACs and related anatomical structures [14,49,88]. In addition, the specific relationship between those two vulnerable anatomical structures (NPCs and ACs) in anterior maxilla was estimated by Vasiljevic and coworkers [49], confirming that the described relationship significantly depends on the NPC shape.

It has been confirmed that the NPC's and ACs' localization could be a limiting factor for dental implant placement [14,89]. The orthognathic surgical interventions, such as Le Fort 1, require examination of anatomical structures and careful treatment planning to avoid neurovascular complications [90]. From the point of view of implantology, Botermans and coworkers reported that a secure zone between the NPC and the implant is required [48]. However, several virtual implant placement studies showed that it was difficult to achieve those recommendations [21,91]. Furthermore, Botermans and collaborators [48] noticed NPC perforation during virtual immediate implant placement in about 53% of cases, while Jia and colleagues [91] showed slightly above 16%. Also, the damage toACs during implant placement is described in the literature [89]. It is confirmed that the damage to anatomical structures in the anterior maxilla could be followed by several complications, such as non-integration of a dental implant, mucosa necrosis, pain, paresthesia, hemorrhage, the sensation of the burning head in the occipital region, and neuropathy [89,92].

Summarizing the algorithm presented in Figure 5, it is obvious that the patients with a banana NPC shape represent the most vulnerable group for immediate implant placement. On the other hand, the morphometric characteristics of the anterior maxilla in subjects with a cylindrical NPC shape are considered to require additional interventions (such as bone grafting) in order to qualify for immediate implant placement. Hourglass and funnel shapes of the NPC, according to our previous results, allow sufficient operating space for surgical interventions. In order to achieve adequate morphometric conditions for the immediate implant placement, especially in patients with a banana NPC shape, several

additional surgical interventions (such as bone augmentation and NPC exploration) have been proposed [82,83]. Also, it could be considered to use NPC as an implant place [83,84]. Furthermore, it was suggested by Singhal and coworkers [85] to use surgical guides for precise implant placement into nasopalatine foramen. In patients with a funnel NPC shape, simultaneous use of surgical guides during implant insertion has been recommended [86].

As seen in Figure 5, the presence of ACs should be considered as an absolute contraindication for immediate implant placement. So, the clinicians should follow Shelley's [93] recommendation that in those cases there is a need for other therapeutic options, such as a realistic fixed alternative (adhesive cantilever bridge), in order to avoid potentially damaging implant therapy

Because the posterior maxillary parts are often exposed to several [94–99] surgical interventions (such as implant placement therapy, Le Fort I osteotomy, sinus surgery and sinus lift elevation, cyst enucleation, tumor extirpation, surgical tooth extraction, and present donor site area), the accurate morphometric analysis of CBCT images is required for reliable planning.

The anatomical structures in posterior maxillary parts show high variability [100–102]. From the clinical point of view, IRS has been frequently evaluated as the ideal place for implants [63,103]. Numerous advantages of implant placement in maxillary molars IRS are described, such as the possibility of achieving primary implant stability, adequate force distribution, and plaque control [104,105]. On the other hand, anatomical challenges, as well as the differences between implant diameter and post-extractive alveoli, quality and quantity of bone, root length and configuration, the root trunk height, and roots' divergence, could make surgical interventions more difficult [67,106–109]. Several IRS classifications according to the different criteria have been offered in the literature [63,64]. Namely, Bleyan and collaborators [64] described four categories based on the IRS width (after tooth extraction), as follows: S-I—septum initial width above 4 mm; S-II—septum initial width 3–4 mm; S-III—septum initial width 2–3 mm; and S-IV—septum initial width below 2 mm or no septal bone present. On the other hand, Milenkovic and coworkers [63] defined five IRS shapes based on linear measurements and visual impressions (arrow-, boat-, drop-, palatal-convergence-, and buccal-convergence-shaped) by analyzing CBCT images. However, Smith and colleagues [65] estimated the relationship between the implant and the IRS and noticed three categories: type A sockets (alveoli have sufficient septal bone, which circumferentially surrounds the coronal implant part), type B sockets (the septal bone does not cover the total implant surface, but it is enough to achieve primary implant stability), and the least, type C (has an insufficient septal bone to stabilize the implant without engaging the socket wall).

In post-extractive alveoli, clinicians could also use one of the root cavities to insert the implant in order to achieve primary implant fixation, but it does not meet the requirements for the correct prosthetic implant position [110]. However, previous studies reported that IRS presents the ideal implant site from a prosthetic view [111]. It is not surprising that Rajkovic Pavlovic and coworkers [112] emphasized the importance of radiological IRS evaluation in implant placement planning due to the fact that primary implant stability is determined by the alveoli architecture [113]. In order to obtain better insights into IRS morphological characteristics, Milenkovic and coworkers [63] presented criteria for the classification of five IRS shapes. As presented in Figure 7, the minimal clinical margin for achieving the primary implant stability could not be established only for the drop-shaped IRS, according to the criterion of IRS width. In contrast, this indicator for the primary implant stability in the second molars was achieved only in the boat IRS shape. According to the implant height, as the criterion necessary to achieve implant stability, none of the IRS shapes allows for successful implant placement.

Although previous analyses do not look optimistic from the point of implant placement success, it should be noted that clinicians have a plethora of possibilities to achieve the final success of implant stability by applying additional interventions. Those interventions may be performed prior to implant placement, simultaneously, and/or following the

standard implant placement procedure. Some of them are aimed at increasing the IRS width, while the others are recommended for the enlargement of the IRS height. As previously commented, both goals have to be achieved. However, the final success of those procedures accompanied with the implant placement is still under evaluation.

Considering the procedures for the enhancement of IRS width, it should be noticed that osseodensification is a novel method of biomechanical bone preparation in order to achieve improvement in better implant stability when compared to the standard drill [69]. Hence, in the clinical study conducted by Bleyan and coworkers [64], theosseodensification method to improve IRS dimensions was used. They reported the success of implant therapy by means of a 93.1% survival rate at the 12-month follow-up (135/145 implants). Another surgical technique that improves the post-extractive alveoli volume is socket grafting [114–117]. There are numerous materials for filling the gap between implants and alveoli described in the literature [118–120]. The clinical studies confirmed the success of implant therapy by substituting the insufficient implant sites [65,121].

In cases with insufficient bone height, the sinus lift procedure aims to improve vertical bone dimensions below the maxillary sinus in order to provide the possibility of implant placement [122]. Also, the sinus membrane perforation risk could be reduced through this procedure while simultaneously achieving primary implant stability [123]. On the other hand, the dimensions of membrane perforation play an important role in implant placement success [124,125] Thus, Lombardo and coworkers concluded that internal sinus lift presented a small risk of membrane perforation and stable bone around implants with a high rate of success at mid-term follow-up for atrophic maxilla [126].

The mentioned procedures aimed to enhance IRS width and IRS height, and in relation to the analysis presented in the study that analyzed IRS shapes, it is worth noting that CBCT images' morphometric analysis allows for the achievement of exact morphometric parameters that can lead to better planning of interventions in the maxillary molar region.

On the other hand, modern implant therapy includesshort implants with wide threads, such as AnyRidge implants (Anyridge®, Megagen, South Korea) [127]. Numerous studies concluded that using this implant type may achieve high primary stability in immediate implant placement for the maxillary posterior region [128,129].

6. Conclusions

Taken altogether, the impact of the methodological approach based on CBCT image analysis of maxilla, as presented in this summary of our recent studies, is manifested by achieving more reliable recommendations for performing certain interventions in the maxillary region. Summarizing the proposed operating procedures, according to our recent investigations based on the potential usefulness of CBCT-based diagnostic procedures in planning some specific interventions in the described regions of interest, it seems that the following can be stated:

- The possibility for immediate implant placement may be affected by the NPC shape in the anterior maxilla, while the presence of ACs, in general, may increase the incidence of immediate implant placement complications;
- The variations in IRS characteristics may be considered important criteria for choosing the implant properties required for successful immediate implant placement.

The presented relationships of potential clinical importance may be considered as tentative factors for exclusion criteria under the described circumstances. Furthermore, in the case that there are no absolute contraindications for the interventions in this region, the use of the proposed methodology allows for better intervention planning by means of predefining optimal procedures and quantification of the extent of accompanied treatments.

7. Future Directions

The recent literature provides exact data on the anatomical configuration of the upper jaw that may affect implant placement. However, subsequent studies could be directed towards virtual implant placement in order to obtain more precise insight into the relation-

ship between the implant and vulnerable anatomical structures, such as the NPC, ACs, and maxillary sinus membrane. Beside gold standards for implant macrodesign, using virtual planning software for implant surgery with a different macrodesign should also be examined, as well as the relationship between such a design and the aforementioned anatomical structure.

Abbreviations

CBCT	Cone beam computed tomography
NPC	Nasopalatine canal
ACs	Accessory canals
IRS	Interradicular septum

References

1. Von Arx, T.; Lozanoff, S. *Clinical Oral Anatomy*; Springer: Cham, Switzerland, 2017. [CrossRef]
2. Scarfe, W.C.; Farman, A.G. What is cone-beam CT and how does it work? *Dent. Clin. N. Am.* **2008**, *52*, 707–730. [CrossRef] [PubMed]
3. Kumar, M.; Shanavas, M.; Sidappa, A.; Kiran, M. Cone beam computed tomography—Know its secrets. *J. Int. Oral Health* **2015**, *7*, 64–68. [PubMed]
4. Hashimoto, K.; Kawashima, S.; Araki, M.; Iwai, K.; Sawada, K.; Akiyama, Y. Comparison of image performance between cone-beam computed tomography for dental use and four-row multidetector helical CT. *J. Oral Sci.* **2006**, *48*, 27–34. [CrossRef] [PubMed]
5. Shahbazian, M.; Vandewoude, C.; Wyatt, J.; Jacobs, R. Comparative assessment of panoramic radiography and CBCT imaging for radiodiagnostics in the posterior maxilla. *Clin. Oral Investig.* **2014**, *18*, 293–300. [CrossRef] [PubMed]
6. DeVos, W.; Casselman, J.; Swennen, G.R. Cone beam computerized tomography (CBCT) imaging of oral and maxillofacial region: A systemic review of literature. *Int. J. Oral Maxillofac. Surg.* **2009**, *38*, 609–625. [CrossRef] [PubMed]
7. Orhan, K.; KusakciSeker, B.; Aksoy, S.; Bayindir, H.; Berberoğlu, A.; Seker, E. Cone beam CT evaluation of maxillary sinus septa prevalence, height, location and morphology in children and an adult population. *Med. Princ. Pract.* **2013**, *22*, 47–53. [CrossRef] [PubMed]
8. Ortiz-Puigpelat, O.; Lázaro-Abdulkarim, A.; de Medrano-Reñé, J.M.; Gargallo-Albiol, J.; Cabratosa-Termes, J.; Hernández-Alfaro, F. Influence of Implant Position in Implant-Assisted Removable Partial Denture: A Three-Dimensional Finite Element Analysis. *J. Prosthodont.* **2019**, *28*, e675–e681. [CrossRef] [PubMed]
9. Loubele, M.; Bogaerts, R.; Van Dijck, E.; Pauwels, R.; Vanheusden, S.; Suetens, P.; Marchal, G.; Sanderink, G.; Jacobs, R. Comparison between effective radiation dose of CBCT and MSCT scanners for dentomaxillofacial applications. *Eur. J. Radiol.* **2009**, *71*, 461–468. [CrossRef] [PubMed]
10. Winter, A.A.; Pollack, A.S.; Frommer, H.H.; Koenig, L. Cone beam volumetric tomography vs. medical CT scanners. *N. Y. State Dent. J.* **2005**, *71*, 28–33.
11. Von Arx, T.; Lozanoff, S.; Bornstein, M.M. Extraoral anatomy in CBCT—A literature review. Part 1: Nasoethmoidal region. *Swiss Dent. J.* **2019**, *129*, 804–815. [CrossRef] [PubMed]
12. Hodez, C.; Griffaton-Taillandier, C.; Bensimon, I. Cone-beam imaging: Applications in ENT. *Eur. Ann. Otorhinolaryngol. Head Neck Dis.* **2011**, *128*, 65–78. [CrossRef] [PubMed]
13. Arnaut, A.; Milanovic, P.; Vasiljevic, M.; Jovicic, N.; Vojinovic, R.; Selakovic, D.; Rosic, G. The Shape of Nasopalatine Canal as a Determining Factor in Therapeutic Approach for Orthodontic Teeth Movement—A CBCT Study. *Diagnostics* **2021**, *11*, 2345. [CrossRef] [PubMed]
14. Milanovic, P.; Selakovic, D.; Vasiljevic, M.; Jovicic, N.U.; Milovanović, D.; Vasovic, M.; Rosic, G. Morphological Characteristics of the Nasopalatine Canal and the Relationship with the Anterior Maxillary Bone—A Cone Beam Computed Tomography Study. *Diagnostics* **2021**, *11*, 915. [CrossRef] [PubMed]

15. Bremke, M.; Leppek, R.; Werner, J.A. Die digitale Volumen tomographie in der HNO-Heilkunde [Digital volume tomography in ENT medicine]. *HNO* **2010**, *58*, 823–832. [CrossRef] [PubMed]

16. Tschopp, M.; Bornstein, M.M.; Sendi, P.; Jacobs, R.; Goldblum, D. Dacryocystography using cone beam CT in patients with lacrimal drainage system obstruction. *Ophthalmic Plast. Reconstr. Surg.* **2014**, *30*, 486–491. [CrossRef] [PubMed]

17. Gaêta-Araujo, H.; Alzoubi, T.; Vasconcelos, K.F.; Orhan, K.; Pauwels, R.; Casselman, J.W.; Jacobs, R. Cone beam computed tomography in dentomaxillofacial radiology: A two-decade overview. *Dentomaxillofac. Radiol.* **2020**, *49*, 20200145. [CrossRef] [PubMed]

18. Dula, K.; Benic, G.I.; Bornstein, M.M.; Dagassan Berndt, D.; Filippi, A.; Hicklin, S.; Kissling-Jeger, F.; Luebbers, H.T.; Sculean, A.; Sequeira-Byron, P.; et al. SADMFR guidelines for the use of cone beam computed tomography/digital volume tomography. *Swiss Dent. J.* **2015**, *125*, 945–953. [CrossRef] [PubMed]

19. Tyndall, D.A.; Price, J.B.; Tetradis, S.; Ganz, S.D.; Hildebolt, C.; Scarfe, W.C. Position statement of the American Academy of Oral and Maxillofacial Radiology on selection criteria for the use of radiology in dental implantology with emphasis on cone beam computed tomography. Oral Surg. *Oral Surg. Oral Med. Oral Pathol. Oral Radiol.* **2012**, *113*, 817–826. [CrossRef] [PubMed]

20. Buser, D.; Chappuis, V.; Belser, U.C.; Chen, S. Implant placement post extraction in esthetic single tooth sites: When immediate, when early, when late? *Periodontology 2000* **2016**, *73*, 84–102. [CrossRef] [PubMed]

21. Alkanderi, A.; Al Sakka, Y.; Koticha, T.; Li, J.; Masood, F.; Suárez-López Del Amo, F. Incidence of nasopalatine canal perforation in relation to virtual implant placement: A cone beam computed tomography study. *Clin. Implant Dent. Relat. Res.* **2020**, *22*, 77–83. [CrossRef] [PubMed]

22. Chan, H.L.; Garaicoa-Pazmino, C.; Suarez, F.; Monje, A.; Benavides, E.; Oh, T.J.; Wang, H.L. Incidence of implant buccal plate fenestration in the esthetic zone: A cone beam computed tomography study. *Int. J. Oral Maxillofac. Implants* **2014**, *29*, 171–177. [CrossRef] [PubMed]

23. Lin, H.H.; Lo, L.J. Three-dimensional computer-assisted surgical simulation and intraoperative navigation in orthognathic surgery: A literature review. *J. Formos. Med. Assoc.* **2015**, *114*, 300–307. [CrossRef] [PubMed]

24. Adolphs, N.; Haberl, E.J.; Liu, W.; Keeve, E.; Menneking, H.; Hoffmeister, B. Virtual planning for craniomaxillofacial surgery—7 Years of experience. *J. Cranio-Maxillofac. Surg.* **2014**, *42*, e289–e295. [CrossRef] [PubMed]

25. Zinser, M.J.; Mischkowski, R.A.; Dreiseidler, T.; Thamm, O.C.; Rothamel, D.; Zöller, J.E. Computer-assisted orthognathic surgery: Waferless maxillary positioning, versatility, and accuracy of an image-guided visualisation display. *Br. J. Oral Maxillofac. Surg.* **2013**, *51*, 827–833. [CrossRef] [PubMed]

26. Alkhayer, A.; Piffkó, J.; Lippold, C.; Segatto, E. Accuracy of virtual planning in orthognathic surgery: A systematic review. *Head Face Med.* **2020**, *16*, 34. [CrossRef] [PubMed]

27. Deporter, D.; EbrahimiDastgurdi, M.; Rahmati, A.; G Atenafu, E.; Ketabi, M. CBCT data relevant in treatment planning for immediate maxillary molar implant placement. *J. Adv. Periodontol. Implant Dent.* **2021**, *2*, 49–55. [CrossRef] [PubMed]

28. Nickenig, H.J.; Eitner, S. Reliability of implant placement after virtual planning of implant positions using cone beam CT data and surgical (guide) templates. *J. Craniomaxillofac. Surg.* **2007**, *4–5*, 207–211. [CrossRef] [PubMed]

29. Ramasamy, M.; Giri; Raja, R.; Subramonian; Karthik; Narendrakumar, R. Implant surgical guides: From the past to the present. *J. Pharm. Bioallied Sci.* **2013**, *1*, S98–S102. [CrossRef] [PubMed]

30. Abdelhamid, A.; Omran, M.; Bakhshalian, N.; Tarnow, D.; Zadeh, H.H. An open randomized controlled clinical trial to evaluate ridge preservation and repair using SocketKAPTM and SocketKAGETM: Part 2—Three-dimensional alveolar bone volumetric analysis of CBCT imaging. *Clin. Oral Implants Res.* **2015**, *27*, 631–639. [CrossRef] [PubMed]

31. Gorla, L.F.; Spin-Neto, R.; Boos, F.B.; Pereira Rdos, S.; Garcia Junior, I.R.; Hochuli-Vieira, E. Use of autogenous bone and beta-tricalcium phosphate in maxillary sinus lifting: A prospective, randomized, volumetric computed tomography study. *Int. J. Oral Maxillofac. Surg.* **2015**, *44*, 1486–1491. [CrossRef] [PubMed]

32. Markovic, A.; Misic, T.; Calvo-Guirado, J.L.; Delgado-Ruiz, R.A.; Janjic, B.; Abboud, M. Two-center prospective, randomized, clinical, and radiographic study comparing osteotome sinus floor elevation with or without bone graft and simultaneous implant placement. *Clin. Implant Dent. Relat. Res.* **2016**, *18*, 873–882. [CrossRef] [PubMed]

33. Kuchler, U.; Chappuis, V.; Gruber, R.; Lang, N.P.; Salvi, G.E. Immediate implant placement with simultaneous guided bone regeneration in the esthetic zone: 10-year clinical and radiographic outcomes. *Clin. Oral Implants Res.* **2016**, *27*, 253–257. [CrossRef] [PubMed]

34. Chen, S.T.; Buser, D. Esthetic outcomes following immediate and early implant placement in the anterior maxilla—A systematic review. *Int. J. Oral Maxillofac. Implants* **2014**, *29*, 186–215. [CrossRef] [PubMed]

35. Misch, C.M.; Jensen, O.T.; Pikos, M.A.; Malmquist, J.P. Vertical bone augmentation using recombinant bone morphogenetic protein, mineralized bone allograft, and titanium mesh: A retrospective cone beam computed tomography study. *Int. J. Oral Maxillofac. Implants* **2015**, *30*, 202–207. [CrossRef] [PubMed]

36. Spin-Neto, R.; Stavropoulos, A.; Coletti, F.L.; Pereira, L.A.; Marcantonio, E., Jr.; Wenzel, A. Remodeling of cortical and corticocancellous fresh-frozen allogenic block bone grafts—A radiographic and histomorphometric comparison to autologous bone grafts. *Clin. Oral Implants Res.* **2015**, *26*, 747–752. [CrossRef] [PubMed]

37. Cho, E.A.; Kim, S.J.; Choi, Y.J.; Kim, K.-H.; Chung, C.J. Morphologic evaluation of the incisive canal and its proximity to the maxillary central incisors using computed tomography images. *Angle Orthod.* **2015**, *86*, 571–576. [CrossRef] [PubMed]

38. Gull, M.A.B.; Maqbool, S.; Mushtaq, M.; Ahmad, A. Evaluation of Morphologic Features and Proximity of Incisive Canal to the Maxillary Central Incisors Using Cone Beam Computed Tomography. *IOSR J. Dent. Med. Sci.* **2018**, *17*, 46–50.

39. Bornstein, M.M.; Balsiger, R.; Sendi, P.; von Arx, T. Morphology of the nasopalatine canal and dental implant surgery: A radiographic analysis of 100 consecutive patients using limited cone-beam computed tomography. *Clin. Oral Implants Res.* **2011**, *22*, 295–301. [CrossRef] [PubMed]

40. Jacobs, R.; Lambrichts, I.; Liang, X.; Martens, W.; Mraiwa, N.; Adriaensens, P.; Gelan, J. Neurovascularization of the anterior jaw bones revisited using high-resolution magnetic resonance imaging. *Oral Surg. Oral Med. Oral Pathol. Oral Radiol. Endod.* **2007**, *103*, 683–693. [CrossRef] [PubMed]

41. Lake, S.; Iwanaga, J.; Kikuta, S.; Oskouian, R.J.; Loukas, M.; Tubbs, R.S. The Incisive Canal: A Comprehensive Review. *Cureus* **2018**, *10*, e3069. [CrossRef] [PubMed]

42. Keith, D.A. Phenomenon of mucous retention in the incisive canal. *J. Oral Surg.* **1979**, *37*, 832–834. [PubMed]

43. Mardinger, O.; Namani-Sadan, N.; Chaushu, G.; Schwartz-Arad, D. Morphologic Changes of the Nasopalatine Canal Related to Dental Implantation: A Radiologic Study in Different Degrees of Absorbed Maxillae. *J. Periodontol.* **2008**, *79*, 1659–1662. [CrossRef] [PubMed]

44. Fukuda, M.; Matsunaga, S.; Odaka, K.; Oomine, Y.; Kasahara, M.; Yamamoto, M.; Abe, S. Three-dimensional analysis of incisive canals in human dentulous and edentulous maxillary bones. *Int. J. Implant Dent.* **2015**, *1*, 12. [CrossRef] [PubMed]

45. Gil-Marques, B.; Sanchis-Gimeno, J.A.; Brizuela-Velasco, A.; Perez-Bermejo, M.; Larrazábal-Morón, C. Differences in the shape and direction-course of the nasopalatine canal among dentate, partially edentulous and completely edentulous subjects. *Anat. Sci. Int.* **2020**, *95*, 76–84. [CrossRef] [PubMed]

46. De Lima, A.C.N.M.; Peniche, D.A.; Coutinho, T.M.C.; Guedes, F.R.; Visconti, M.A.; Risso, P.A. The nasopalatine canal and its relationship with the maxillary central incisors: A cone-beam computed tomography study. *Res. Soc. Dev.* **2021**, *10*, e351101522978. [CrossRef]

47. Etoz, M.; Sisman, Y. Evaluation of the nasopalatine canal and variations with cone-beam computed tomography. *Surg. Radiol. Anat.* **2014**, *36*, 805–812. [CrossRef]

48. Botermans, A.; Lidén, A.; de Carvalho Machado, V.; Chrcanovic, B.R. Immediate Implant Placement in the Maxillary Aesthetic Zone: A Cone Beam Computed Tomography Study. *J. Clin. Med.* **2021**, *10*, 5853. [CrossRef] [PubMed]

49. Vasiljevic, M.; Milanovic, P.; Jovicic, N.; Vasovic, M.; Milovanovic, D.; Vojinovic, R.; Selakovic, D.; Rosic, G. Morphological and Morphometric Characteristics of Anterior Maxilla Accessory Canals and Relationship with Nasopalatine Canal Type-A CBCT Study. *Diagnostics* **2021**, *11*, 1510. [CrossRef] [PubMed]

50. Baena-Caldas, G.; Rengifo-Miranda, H.; Heerera-Rubio, A.; Peckham, X.; Zúñiga, J. Frequency of canalissinuosus and its anatomic variations in cone beam computed tomography images. *Int. J. Morphol.* **2019**, *37*, 852–857. [CrossRef]

51. Machado, V.C.; Chrcanovic, B.R.; Felippe, M.B.; Manhães Júnior, L.R.; de Carvalho, P.S. Assessment of accessory canals of the canalissinuosus: A study of 1000 cone beam computed tomography examinations. *Int. J. Oral Maxillofac. Surg.* **2016**, *45*, 1586–1591. [CrossRef] [PubMed]

52. Von Arx, T.; Lozanoff, S.; Sendi, P.; Bornstein, M.M. Assessment of bone channels other than the nasopalatine canal in the anterior maxilla using limited cone beam computed tomography. *Surg. Radiol. Anat.* **2013**, *35*, 783–790. [CrossRef] [PubMed]

53. Tomrukçu, D.N.; Köse, T.E. Assesment of accessory branches of canalissinuosus on CBCT images. *Med. Oral Patol. Oral Cir. Bucal.* **2020**, *25*, e124–e130. [CrossRef] [PubMed]

54. Wanzeler, A.M.; Marinho, C.G.; Alves Junior, S.M.; Manzi, F.R.; Tuji, F.M. Anatomical study of the canalissinuosus in 100 cone beam computed tomography examinations. *Oral Maxillofac. Surg.* **2015**, *19*, 49–53. [CrossRef] [PubMed]

55. Anatoly, A.; Sedov, Y.; Gvozdikova, E.; Mordanov, O.; Kruchinina, L.; Avanesov, K.; Vinogradova, A.; Golub, S.; Khaydar, D.; Hoang, N.G.; et al. Radiological and Morphometric Features of CanalisSinuosus in Russian Population: Cone-Beam Computed Tomography Study. *Int. J. Dent.* **2019**, *2019*, 2453469. [CrossRef] [PubMed]

56. Manhães Júnior, L.R.; Villaça-Carvalho, M.F.; Moraes, M.E.; Lopes, S.L.; Silva, M.B.; Junqueira, J.L. Location and classification of Canalissinuosus for cone beam computed tomography: Avoiding misdiagnosis. *Braz. Oral Res.* **2016**, *30*, e49. [CrossRef] [PubMed]

57. De Oliveira-Santos, C.; Rubira-Bullen, I.R.; Monteiro, S.A.; León, J.E.; Jacobs, R. Neurovascular anatomical variations in the anterior palate observed on CBCT images. *Clin. Oral Implants Res.* **2013**, *24*, 1044–1048. [CrossRef] [PubMed]

58. Hwang, K.G.; Park, C.J. Ideal implant positioning in an anterior maxillary extraction socket by creating an apico-palatal guiding slot: A technical note. *Int. J. Oral Maxillofac. Implants* **2008**, *23*, 121–122. [PubMed]

59. Greenstein, G.; Tarnow, D. The mental foramen and nerve: Clinical and anatomical factors related to dental implant placement: A literature review. *J. Periodontol.* **2006**, *77*, 1933–1943. [CrossRef] [PubMed]

60. Sharma, S.; Narkhede, S.; Sonawane, S.; Gangurde, P. Evaluation of Patient's Personal Reasons and Experience with Orthodontic Treatment. *J. Int. Oral Health* **2013**, *5*, 78–81. [PubMed]

61. Chung, C.J.; Nguyen, T.; Lee, J.; Kim, K. Incisive canal remodelling following maximum anterior retraction reduces apical root resorption. *Orthod. Craniofacial. Res.* **2021**, *24*, 59–65. [CrossRef] [PubMed]

62. Pavlovic, Z.R.; Milanovic, P.; Vasiljevic, M.; Jovicic, N.; Arnaut, A.; Colic, D.; Petrovic, M.; Stevanovic, M.; Selakovic, D.; Rosic, G. Assessment of Maxillary Molars Interradicular Septum Morphological Characteristics as Criteria for Ideal Immediate Implant Placement—The Advantages of Cone Beam Computed Tomography Analysis. *Diagnostics* **2022**, *12*, 1010. [CrossRef] [PubMed]

63. Milenkovic, J.; Vasiljevic, M.; Jovicic, N.; Milovanovic, D.; Selakovic, D.; Rosic, G. Criteria for the Classification of the Interradicular Septum Shape in Maxillary Molars with Clinical Importance for Prosthetic-Driven Immediate Implant Placement. *Diagnostics* **2022**, *12*, 1432. [CrossRef] [PubMed]

64. Bleyan, S.; Gaspar, J.; Huwais, S.; Schwimer, C.; Mazor, Z.; Mendes, J.J.; Neiva, R. Molar Septum Expansion with Osseodensification for Immediate Implant Placement, Retrospective Multicenter Study with Up-to-5-Year Follow-Up, Introducing a New Molar Socket Classification. *J. Funct. Biomater.* **2021**, *12*, 66. [CrossRef] [PubMed]

65. Smith, R.B.; Tarnow, D.P. Classification of molar extraction sites for immediate dental implant placement: Technical note. *Int. J. Oral Maxillofac. Implants* **2013**, *28*, 911–916. [CrossRef] [PubMed]

66. Agostinelli, C.; Agostinelli, A.; Berardini, M.; Trisi, P. Anatomical and Radiologic Evaluation of the Dimensions of Upper Molar Alveoli. *Implant Dent.* **2018**, *27*, 171–176. [CrossRef] [PubMed]

67. Padhye, N.; Shirsekar, V. Tomographic evaluation of mandibular molar alveolar bone for immediate implant placement—A retrospective cross-sectional study. *Clin. Oral Implants Res.* **2019**, *30*, 265. [CrossRef]

68. Nunes, L.S.; Bornstein, M.M.; Sendi, P.; Buser, D. Anatomical characteristics and dimensions of edentulous sites in the posterior maxillae of patients referred for implant therapy. *Int. J. Periodontics Restor. Dent.* **2013**, *33*, 337–345. [CrossRef] [PubMed]

69. Pai, U.Y.; Rodrigues, S.J.; Talreja, K.S.; Mundathaje, M. Osseodensification—A novel approach in implant dentistry. *J. Indian Prosthodont. Soc.* **2018**, *18*, 196–200. [CrossRef] [PubMed]

70. Alhayati, J.Z.; Al-Anee, A.M. Evaluation of crestal sinus floor elevations using versah burs with simultaneous implant placement, at residual bone height ≥2.0_<6.0 mm. A prospective clinical study. *Oral Maxillofac. Surg.* **2023**, *27*, 325–332. [CrossRef] [PubMed]

71. Demirkol, N.; Demirkol, M. The Diameter and Length Properties of Single Posterior Dental Implants: A Retrospective Study. *Cumhur. Dent. J.* **2019**, *22*, 276–282. [CrossRef]

72. Thirunavakarasu, R.; Arun, M.; Abhinav, R.P.; Ganesh, B.S. Commonly Used Implant Dimensions in the Posterior Maxilla—A Retrospective Study. *J. Long-Term Eff. Med. Implants* **2022**, *32*, 25–32. [CrossRef] [PubMed]

73. Ghoncheh, Z.; Zade, B.M.; Kharazifard, M.J. Root Morphology of the Maxillary First and Second Molars in an Iranian Population Using Cone Beam Computed Tomography. *J. Dent.* **2017**, *14*, 115–122.

74. Wang, H.M.; Shen, J.W.; Yu, M.F.; Chen, X.Y.; Jiang, Q.H.; He, F.M. Analysis of facial bone wall dimensions and sagittal root position in the maxillary esthetic zone: A retrospective study using cone beam computed tomography. *Int. J. Oral Maxillofac. Implants* **2014**, *29*, 1123–1129. [CrossRef] [PubMed]

75. Miyamoto, Y.; Obama, T. Dental cone beam computed tomography analyses of postoperative labial bone thickness in maxillary anterior implants: Comparing immediate and delayed implant placement. *Int. J. Periodontics Restor. Dent.* **2011**, *31*, 215–225.

76. Grunder, U.; Gracis, S.; Capelli, M. Influence of the 3-D bone-to-implant relationship on esthetics. *Int. J. Periodontics Restor. Dent.* **2005**, *25*, 113–119.

77. Zhan, W.; Skrypczak, A.; Weltman, R. Anterior maxilla alveolar ridge dimension and morphology measurement by cone beam computerized tomography (CBCT) for immediate implant treatment planning. *BMC Oral Health* **2015**, *15*, 65.

78. Safi, Y.; Moshfeghi, M.; Rahimian, S.; Kheirkhahi, M.; Manouchehri, M.E. Assessment of Nasopalatine Canal Anatomic Variations Using Cone Beam Computed Tomography in a Group of Iranian Population. *Iran. J. Radiol.* **2017**, *14*, e13480. [CrossRef]

79. Bahşi, I.; Orhan, M.; Kervancıoğlu, P.; Yalçın, E.D.; Aktan, A.M. Anatomical evaluation of nasopalatine canal on cone beam computed tomography images. *Folia. Morphol.* **2019**, *78*, 153–162. [CrossRef] [PubMed]

80. Güncü, G.N.; Yıldırım, Y.D.; Yılmaz, H.G.; Galindo-Moreno, P.; Velasco-Torres, M.; Al-Hezaimi, K.; Al-Shawaf, R.; Karabulut, E.; Wang, H.L.; Tözüm, T.F. Is there a gender difference in anatomic features of incisive canal and maxillary environmental bone? *Clin. Oral Implants Res.* **2013**, *24*, 1023–1026. [CrossRef] [PubMed]

81. Jornet, P.L.; Boix, P.P.; Perez, A.S.; Boracchia, A. Morphological Characterization of the Anterior Palatine Region Using Cone Beam Computed Tomography. *Clin. Implant Dent. Relat. Res.* **2014**, *17*, 459–464.

82. Chen, K.; Li, Z.; Liu, X.; Liu, Q.; Chen, Z.; Sun, Y.; Chen, Z.; Huang, B. Immediate Implant Placement with Buccal Bone Augmentation in the Anterior Maxilla with Thin Buccal Plate: A One-Year Follow-Up Case Series. *J. Prosthodont.* **2021**, *30*, 473–480. [CrossRef] [PubMed]

83. Bodereau, E.F.; Flores, V.Y.; Naldini, P.; Torassa, D.; Tortolini, P. Clinical Evaluation of the Nasopalatine Canal in Implant-Prosthetic Treatment: A Pilot Study. *Dent. J.* **2020**, *8*, 30. [CrossRef]

84. Scher, E.L. Use of the incisive canal as a recipient site for root form implants: Preliminary clinical reports. *Implant Dent.* **1994**, *1*, 38–41. [CrossRef] [PubMed]

85. Singhal, M.K.; Dandriyal, R.; Aggarwal, A.; Agarwal, A.; Yadav, S.; Baranwal, P. Implant Placement into the Nasopalatine Foramen: Considerations from Anatomical and Surgical Point of View. *Ann. Maxillofac. Surg.* **2018**, *2*, 347–351. [CrossRef] [PubMed]

86. Gargallo-Albiol, J.; Barootchi, S.; Marqués-Guasch, J.; Wang, H.L. Fully Guided Versus Half-Guided and Freehand Implant Placement: Systematic Review and Meta-analysis. *Int. J. Oral Maxillofac. Implants* **2020**, *35*, 1159–1169. [CrossRef] [PubMed]

87. Yeap, C.W.; Danh, D.; Chan, J.; Parashos, P. Examination of canalis sinuosus using cone beam computed tomography in an Australian population. *Aust. Dent. J.* **2022**, *67*, 249–261. [CrossRef] [PubMed]

88. Milanovic, P.; Vasiljevic, M. Gender Differences in the Morphological Characteristics of the Nasopalatine Canal and the Anterior Maxillary Bone—CBCT Study. *Serb. J. Exp. Clin. Res.* **2021**. [CrossRef]

89. Rosano, G.; Testori, T.; Clauser, T.; Massimo Del Fabbro, M. Management of a neurological lesion involving Canalis Sinuosus: A case report. *Clin. Implant Dent. Relat. Res.* **2021**, *23*, 149–155. [CrossRef] [PubMed]

90. Garg, S.; Kaur, S. Evaluation of Post-operative Complication Rate of Le Fort I Osteotomy: A Retrospective and Prospective Study. *J. Maxillofac. Oral Surg.* **2014**, *13*, 120–127. [CrossRef] [PubMed]

91. Jia, X.; Hu, W.; Meng, H. Relationship of central incisor implant placement to the ridge configuration anterior to the nasopalatine canal in dentate and partially edentulous individuals: A comparative study. *PeerJ* **2015**, *3*, e1315. [CrossRef] [PubMed]

92. McCrea, S.J.J. Aberrations Causing Neurovascular Damage in the Anterior Maxilla during Dental Implant Placement. *Case Rep. Dent.* **2017**, *2017*, 5969643. [CrossRef] [PubMed]

93. Shelley, A.; Tinning, J.; Yates, J.; Horner, K. Potential neurovascular damage as a result of dental implant placement in the anterior maxilla. *Br. Dent. J.* **2019**, *226*, 657–661. [CrossRef] [PubMed]

94. Salehinejad, J.; Saghafi, S.; Zare-Mahmoodabadi, R.; Ghazi, N.; Kermani, H. Glandular odontogenic cyst of the posterior maxilla. *Arch. Iran Med.* **2011**, *14*, 416–418. [PubMed]

95. Khojasteh, A.; Nazeman, P.; Tolstunov, L. Tuberosity-alveolar block as a donor site for localized augmentation of the maxilla: A retrospective clinical study. *Br. J. Oral Maxillofac. Surg.* **2016**, *54*, 950–955. [CrossRef] [PubMed]

96. Lim, A.A.; Wong, C.W.; Allen, J.C., Jr. Maxillary third molar: Patterns of impaction and their relation to oroantral perforation. *J. Oral Maxillofac. Surg.* **2012**, *70*, 1035–1039. [CrossRef] [PubMed]

97. Lorenz, J.; Blume, M.; Korzinskas, T.; Ghanaati, S.; Sader, R.A. Short implants in the posterior maxilla to avoid sinus augmentation procedure: 5-year results from a retrospective cohort study. *Int. J. Implant. Dent.* **2019**, *5*, 3. [CrossRef] [PubMed]

98. Cheung, L.K.; Fung, S.C.; Li, T.; Samman, N. Posterior maxillary anatomy: Implications for Le Fort I osteotomy. *Int. J. Oral Maxillofac. Surg.* **1998**, *27*, 346–351. [CrossRef] [PubMed]

99. Arul, A.S.; Verma, S.; Arul, A.S.; Verma, R. Infiltrative odontogenic myxoma of the posterior maxilla: Report of a case. *J. Nat. Sci. Biol. Med.* **2013**, *4*, 484–487. [CrossRef] [PubMed]

100. Benic, G.I.; Elmasry, M.; Hammerle, C.H. Novel digital imaging techniques to assess the outcome in oral rehabilitation with dental implants: A narrative review. *Clin. Oral Implants Res.* **2015**, *26*, 86–96. [CrossRef] [PubMed]

101. Whyte, A.; Boeddinghaus, R. The maxillary sinus: Physiology, development and imaging anatomy. *Dentomaxillofac. Radiol.* **2019**, *48*, 20190205. [CrossRef] [PubMed]

102. Stanley, J.N. Wheeler's Dental Anatomy. In *Physiology and Occlusion*, 9th ed.; Saunders Elsevier: St. Louis, MO, USA, 2010.

103. Rodriguez-Tizcareño, M.H.; Bravo-Flores, C. Anatomically guided implant site preparation technique at molar sites. *Implant Dent.* **2009**, *5*, 393–401. [CrossRef] [PubMed]

104. Prosper, L.; Crespi, R.; Valenti, E.; Capparé, P.; Gherlone, E. Five-year follow-up of wide-diameter implants placed in fresh molar extraction sockets in the mandible: Immediate versus delayed loading. *Int. J. Oral Maxillofac. Implants* **2010**, *25*, 607–612. [PubMed]

105. Iglesia-Puig, M.A.; Solana, F.J.; Holtzclaw, D.; Toscano, N. Immediate Implant Considerations for Interradicular Bone in Maxillary Molars: Case Reports. *J. Implant Adv. Clin. Dent.* **2012**, *4*, 19–31.

106. Atieh, M.A.; Payne, A.G.; Duncan, W.J.; de Silva, R.K.; Cullinan, M.P. Immediate placement or immediate restoration/loading of single implants for molar tooth replacement: A systematic review and meta-analysis. *Int. J. Oral Maxillofac. Implants* **2010**, *25*, 401–415. [PubMed]

107. Peñarrocha, M.; Uribe, R.; Balaguer, J. Immediate implants after extraction. A review of the current situation. A review of the current situation. *Med. Oral* **2004**, *9*, 234–242. [PubMed]

108. McAllister, B.S.; Haghighat, K. Bone augmentation techniques. *J. Periodontol.* **2007**, *78*, 377–396. [CrossRef] [PubMed]

109. Rominger, J.W.; Triplett, R.G. The use of guided tissue regeneration to improve implant osseointegration. *J. Oral Maxillofac. Surg.* **1994**, *52*, 106–112. [CrossRef] [PubMed]

110. Almog, D.M.; Sanchez, R. Correlation between planned prosthetic and residual bone trajectories in dental implants. *J. Prosthet. Dent.* **1999**, *81*, 562–567. [CrossRef] [PubMed]

111. Shokry, M.M.; Taalab, M.R. Immediate implant placement through inter-radicular bone drilling before versus after roots extraction in mandibular molar area (a randomized controlled clinical study). *Egypt. Dent. J.* **2022**, *68*, 1377–1388. [CrossRef]

112. Pavlovic, Z.R.; Petrovic, M. Morphological Characteristics of Maxillary Molars Interradicular Septum and Clinical Implications—What Do We Know So Far? *Serb. J. Exp. Clin. Res.* **2022**. [CrossRef]

113. Sayed, A.J.; Shaikh, S.S.; Shaikh, S.Y.; Hussain, M.A. Interradicular bone dimensions in primary stability of immediate molar implants—A cone beam computed tomography retrospective analysis. *Saudi Dent. J.* **2021**, *33*, 1091–1097. [CrossRef] [PubMed]

114. Avila-Ortiz, G.; Elangovan, S.; Kramer, K.W.; Blanchette, D.; Dawson, D.V. Effect of alveolar ridge preservation after tooth extraction: A systematic review and meta-analysis. *J. Dent. Res.* **2014**, *93*, 950–958. [CrossRef] [PubMed]

115. Ohba, S.; Sumita, Y.; Nakatani, Y.; Noda, S.; Asahina, I. Alveolar bone preservation by a hydroxyapatite/collagen composite material after tooth extraction. *Clin. Oral Investig.* **2019**, *23*, 2413–2419. [CrossRef] [PubMed]

116. Covani, U.; Giammarinaro, E.; Marconcini, S. Alveolar socket remodeling: The tug-of-war model. *Med. Hypotheses* **2020**, *142*, 109746. [CrossRef] [PubMed]

117. Covani, U.; Giammarinaro, E.; Panetta, D.; Salvadori, P.A.; Cosola, S.; Marconcini, S. Alveolar Bone Remodeling with or without Collagen Filling of the Extraction Socket: A High-Resolution X-ray Tomography Animal Study. *J. Clin. Med.* **2022**, *11*, 2493. [CrossRef]

118. Lekovic, V.; Camargo, P.M.; Klokkevold, P.R.; Weinlaender, M.; Kenney, E.B.; Dimitrijevic, B.; Nedic, M. Preservation of alveolar bone in extraction sockets using bioabsorbable membranes. *J. Periodontol.* **1998**, *69*, 1044–1049. [CrossRef] [PubMed]

119. Wu, D.; Zhou, L.; Lin, J.; Chen, J.; Huang, W.; Chen, Y. Immediate implant placement in anterior teeth with grafting material of autogenous tooth bone vs xenogenic bone. *BMC Oral Health* **2019**, *19*, 266. [CrossRef] [PubMed]

120. Zaki, J.; Yusuf, N.; El-Khadem, A.; Scholten, R.J.P.M.; Jenniskens, K. Efficacy of bone-substitute materials use in immediate dental implant placement: A systematic review and meta-analysis. *Clin. Implant Dent. Relat. Res.* **2021**, *23*, 506–519. [CrossRef] [PubMed]

121. Artzi, Z.; Parson, A.; Nemcovsky, C.E. Wide-diameter implant placement and internal sinus membrane elevation in the immediate postextraction phase: Clinical and radiographic observations in 12 consecutive molar sites. *Int. J. Oral Maxillofac. Implants* **2003**, *18*, 242–249. [PubMed]

122. Riben, C.; Thor, A. The Maxillary Sinus Membrane Elevation Procedure: Augmentation of Bone around Dental Implants without Grafts-A Review of a Surgical Technique. *Int. J. Dent.* **2012**, *2012*, 105483. [CrossRef] [PubMed]

123. Liu, H.; Liu, R.; Wang, M.; Yang, J. Immediate implant placement combined with maxillary sinus floor elevation utilizing the transalveolar approach and nonsubmerged healing for failing teeth in the maxillary molar area: A randomized controlled trial clinical study with one-year follow-up. *Clin. Implant Dent. Relat. Res.* **2019**, *21*, 462–472. [CrossRef] [PubMed]

124. Díaz-Olivares, L.A.; Cortés-Bretón Brinkmann, J.; Martínez-Rodríguez, N.; Martínez-González, J.M.; López-Quiles, J.; Leco-Berrocal, I.; Meniz-García, C. Management of Schneiderian membrane perforations during maxillary sinus floor augmentation with lateral approach in relation to subsequent implant survival rates: A systematic review and meta-analysis. *Int. J. Implant Dent.* **2021**, *7*, 91. [CrossRef] [PubMed]

125. Testori, T.; Weinstein, T.; Taschieri, S.; Wallace, S.S. Risk factors in lateral window sinus elevation surgery. *Periodontology 2000* **2019**, *81*, 91–123. [CrossRef] [PubMed]

126. Lombardo, G.; Signoriello, A.; Marincola, M.; Liboni, P.; Faccioni, P.; Zangani, A.; D'Agostino, A.; Nocini, P.F. Short and Ultra-Short Implants, in Association with Simultaneous Internal Sinus Lift in the Atrophic Posterior Maxilla: A Five-Year Retrospective Study. *Materials* **2022**, *15*, 7995. [CrossRef] [PubMed]

127. Bechara, S.; Lukosiunas, A.; Dolcini, G.A.; Kubilius, R. Fixed Full Arches Supported by Tapered Implants with Knife-Edge Thread Design and Nanostructured, Calcium-Incorporated Surface: A Short-Term Prospective Clinical Study. *Biomed. Res. Int.* **2017**, *2017*, 4170537. [CrossRef] [PubMed]

128. Hoekstra, J.W.M.; van Oirschot, B.A.; Jansen, J.A.; van den Beucken, J.J. Innovative implant design for continuous implant stability: A mechanical and histological experimental study in the iliac crest of goats. *J. Mech. Behav. Biomed. Mater.* **2021**, *122*, 104651. [CrossRef] [PubMed]

129. Baldi, D.; Lombardi, T.; Colombo, J.; Cervino, G.; Perinetti, G.; Di Lenarda, R.; Stacchi, C. Correlation between Insertion Torque and Implant Stability Quotient in Tapered Implants with Knife-Edge Thread Design. *Biomed. Res. Int.* **2018**, *2018*, 7201093. [CrossRef] [PubMed]